Macromolecules
ARTICLE

Macromolecules **2009**, *42*, 8907–8913 **8907**
DOI: 10.1021/ma901643g

Reduced Cooperative Segmental Motion and Hindered Hydrogen Bonding of Poly(ethylene oxide) Intercalated in Layered Silicates: Deductions Revealed by Simulating ESR Spectra of Spin-Labeled PEO and by XRD, DSC, and TGA Measurements

Yohei Miwa,[†,§] Andrew R. Drews,[‡] and Shulamith Schlick*[,†]

[†]*Department of Chemistry and Biochemistry, University of Detroit Mercy, 4001 West McNichols Road, Detroit, Michigan 48221-3038, and* [‡]*Ford Research and Innovation Center, Ford Motor Company, MD 3179, P.O. Box 2053, Dearborn, Michigan 48121.* [§]*Present address: Mitsubishi Chemical Group Science and Technology Research Center, Inc., Japan.*

Received July 24, 2009; Revised Manuscript Received August 28, 2009

ABSTRACT: The structure and dynamics of poly(ethylene oxide) (MW 400, PEO400) intercalated in the galleries of a layered fluoromica clay were investigated by spin-label electron spin resonance (ESR), XRD, DSC, and TGA. PEO400 was end-labeled by attachment of a nitroxide radical and intercalated in 0.78 nm clay galleries. The ESR spectra of intercalated PEO400 showed two motional components, fast and slow, which were attributed to polymer segments weakly and strongly interacting with the clay interface, respectively, while a single spectral component was measured for bulk PEO400. The rotational diffusion coefficient for the polymer chain segment, R_S, was determined by simulating the temperature variation of the ESR spectra, based on the "macroscopic order with microscopic disorder" (MOMD) model. The effect of the molecular weight was assessed by comparison with the previous study of PEO4000 (PEO4K [Miwa, Y.; et al. *Macromolecules* **2008**, *41*, 4701−4708]. The values of log R_S for bulk PEO400 and PEO4K at 330 K were 8.8 and 7.4, respectively; the higher mobility of bulk PEO400 is considered to be a result of the higher concentration of chain ends, which leads to their enhanced mobility through cooperative motion. In contrast to bulk PEO, the mobility of the spin-labeled intercalated PEO was *not* enhanced, indicating that the cooperative segmental motion of PEO in the galleries is reduced. The smaller A_{zz} value (the ^{14}N hyperfine splitting along the z axis of the $2p_z$ orbital of the unpaired electron) for intercalated PEO400 compared to the bulk polymer was taken as an indication that hydrogen bonding between the nitroxide labels and the hydroxyl chain ends of PEO400 in the galleries is hindered. From these results, it was concluded that interactions between PEO segments are negligible and cooperative segmental motions are reduced in the galleries.

Introduction

The structure and dynamics of poly(ethylene oxide) (PEO) chains intercalated in layered silicate galleries have attracted great interest as a model system to study polymer behavior in nanoscopically confined media.[1−11] In this system the PEO chains are confined in narrow, < 1 nm wide, galleries between the inorganic layers. The unique structure and mobility of intercalated PEO chains compared to bulk PEO are due to limited available space and to the interaction with the charged surface of the inorganic host layers and with interlayer cations.

The intercalated PEO does not show a melting transition in differential scanning calorimetry (DSC), indicating that polymer crystallization is inhibited.[6] The conformation of the intercalated PEO has been discussed in some important papers. A helical conformation of the intercalated PEO was first proposed on the basis of Fourier transform infrared (FTIR) and ^{23}Na and ^{13}C solid-state nuclear magnetic resonance (NMR).[1] However, Harris et al. suggested that long helical sections in intercalated PEO are not possible because of the low trans content demonstrated by double-quantum ^{13}C solid-state NMR.[7] Wu and Lerner proposed the existence of all-trans PEO conformations due to adsorption of polymer layers on the inorganic host surfaces.[2] However, Bujdák et al. claimed that a highly ordered structure is improbable from energetic considerations.[8] Recently, Giannelis and co-workers decided on disordered and liquidlike structure of PEO on the basis of computer simulations, ^{7}Li, ^{23}Na, and ^{2}H solid-state NMR, and X-ray diffraction (XRD).[3,4,9,12]

The dynamics of PEO intercalated in clay galleries has been studied by solid-state NMR,[3−5] thermally stimulated current (TSC),[6] dielectric spectroscopy,[13,14] and computer simulations.[9,12,15] As the glass transition is known as a relaxation mode based on cooperative motions of polymer segments,[16] its absence indicates that segmental cooperative motions are hindered in the galleries. TSC measurements, however, showed a broad relaxation starting at about the PEO glass transition temperature (T_g = 218 K) up to ≈333 K, which was characterized by a very low activation energy, E_a.[6] The authors tentatively concluded that TSC is detecting an inherently noncooperative segment motion of the intercalated PEO. Elmahdy et al. detected by dielectric spectroscopy an accelerated segmental dynamics of PEO intercalated in clay galleries that followed an Arrhenius temperature dependence with a single activation energy, while the segmental relaxation of bulk PEO was better explained with two activation energies based on the Vogel−Fulcher−Tammann equation.[13,14] The authors proposed that the higher mobility of intercalated PEO compared to bulk PEO may be due to smaller cooperative region for the intercalated PEO. The ^{2}H NMR line shapes of intercalated deuterated PEO (*d*-PEO) suggested two differences compared to bulk PEO: evidence for enhanced chain

*Corresponding author. E-mail: schlicks@udmercy.edu.

Published on Web 09/18/2009

mobility from the appearance of the central peak at a lower temperature (250 K) compared to bulk PEO (270 K), and the presence of two spectral components, fast and slow, at 340 K only in the nanocomposite; bulk *d*-PEO showed only the fast relaxing component.[3−5] This latter result indicated that the mobility of some segments in intercalated PEO was low even at the high temperature. Computer simulations showed a coexistence of fast and slow segmental relaxations and determined a higher segmental density with a slower segmental relaxation near the inorganic areas.[9,12,15] At higher temperatures the number of cations coordinated to the PEO oxygens decreases, leading to the increase of the relative intensity of the fast spectral component. Moreover, lower segmental density of intercalated PEO than the bulk PEO was demonstrated.

Electron spin resonance (ESR) based on spin-label and spin-probe techniques has been used recently to obtain detailed information on the local environment and dynamics on time scales in the range $10^{-11}-10^{-7}$ s in polymer/inorganic nanocomposites:[17−19] Brik et al. reported the first spin-label study, on PEO/silica nanocomposites, and reported that the polymer motion was hindered in the vicinity of the silica "nodes", a result that was verified by ^{13}C NMR.[17] Jeschke and his group studied the dynamics of a spin-labeled surfactant in organically modified silicates and their composites with polystyrene using CW and pulsed ESR techniques as well as ^{31}P MAS NMR.[18] We have reported on the direct effect of the clay on the intercalated polymer in a spin-label study of exfoliated poly(methyl acrylate) (PMA)/synthetic fluoromica (Somasif) nanocomposites.[19]

Recently, we have applied the ESR spin-label technique to determine the molecular mobility of PEO with a molecular weight of 4K (PEO4K) intercalated in clay galleries.[20] The temperature variation of the ESR spectra was simulated based on the "macroscopic order with microscopic disorder" (MOMD) model, and the mobility of the intercalated PEO was determined. As the PEO4K was intercalated in narrow (0.33 nm) clay galleries, the ESR spectra indicated a very low segmental mobility even at high temperature, 410 K, which was attributed to the strong polymer interaction with the charged silicate platelets. In wider (0.83 nm) galleries, however, the parameters used to simulate the ESR spectra of the nitroxide labels reflected a lowering of the PEO segmental density: In this sample, the ESR spectrum consisted of two distinct contributions from slow and fast motional components, and the relative intensity of the fast component increased with an increase in temperature. These slow and fast motional components for the intercalated PEO were in good agreement with the results indicated by NMR and computer simulations.[3−5,9,12,15] The two spectral components were attributed to segments located close to, and away from, the polar solid walls in the gallery, respectively. Interestingly, the activation energy of the segmental motion in the fast motional component was *lower* compared to that of bulk PEO. The low segmental density and reduced cooperative motion with neighboring segments in the gallery were considered as the main factors leading to the fast PEO chain motion with a low activation energy.

We present a study of the structure and dynamics of PEO having a molecular weight of 400 (PEO400) intercalated in clay galleries, based on the spin-label ESR method that was also used in our previous work.[20] In the bulk, the spin-labeled PEO400 (SLPEO400) showed much higher mobility and larger A_{zz} value than PEO4K, a result that is most likely due to the higher concentration of chain ends (A_{zz} is the ^{14}N hyperfine splitting along the z axis of the $2p_z$ orbital of the unpaired electron). The large A_{zz} value is mainly a result of the hydrogen bonding between hydroxyl groups at the chain ends and the nitroxide labels. The degree of the hydrogen bonding for the intercalated PEO400 was estimated from the A_{zz} value. On the other hand, the enhanced mobility with an increase in the concentration of chain ends indicated that the spin-labeled sites moved cooperatively with the mobile chain ends: The enhanced mobility of the spin-labeled sites with a decrease in a molecular weight is evidence for the cooperative motion with other segments. Therefore, the effect of the molecular weight on the dynamics of the intercalated PEO allowed a qualitative estimate of the degree of cooperative motions for PEO segments in the clay galleries.

Chart 1. Chemical Structure of Spin-Labeled PEO

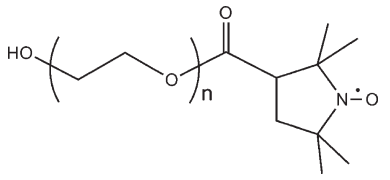

Experimental Section

Materials. Poly(ethylene oxide) having the number-average molecular weight $M_n = 400$ (PEO400) was purchased from Aldrich Chemical Co., Ltd. Anhydrous pyridine (99.8%), thionyl chloride (≥99%), 3-(carboxy)-2,2,5,5-tetramethyl-1-pyrrolidinyloxy (3-carboxy-PROXYL), 4-hydroxy-2,2,6,6-tetramethylpiperidine-1-oxyl (TEMPOL), deionized water (CHROMASOLV), toluene (≥99.5%), and hexanes (99.9%) were also from Aldrich and used as received. Benzene (≥99.5%, Aldrich) was dried with molecular sieves (8−12 mesh, beads effective pore size 10 Å, Fisher Scientific Co.) and calcium hydride (Eastman Kodak Co.). Synthetic fluoromica (Somasif ME-100) was supplied by CO-OP Chemical Co., Ltd., Japan. The chemical composition of Somasif was $Na_{0.66}Mg_{2.68}(Si_{3.98}Al_{0.02})O_{10.02}F_{1.96}$, and the cationic exchange capacity was 115 mequiv/g.[21]

Synthesis of Spin-Labeled PEO400. Before spin-labeling, PEO400 was dialyzed (Bio Design Dialysis tubing #D102) in water for 1 day with water refreshed every several hours and dried at 323 K for 48 h in vacuum after excess water was evaporated. The chain end of PEO was spin-labeled via esterification with 3-carboxy-PROXYL, as described in detail in ref 20. The benzene solution of the spin-labeled polymer (SLPEO400) was added to a large amount of hexane containing 3 vol % of pyridine. The precipitated SLPEO400 was collected and dried at 323 K in vacuum for 24 h; this procedure was repeated five times. Then SLPEO400 was dialyzed in water, as above for the original PEO400. After the large amount of water was evaporated, SLPEO400 was dried at 323 K in vacuum for 48 h and admixed with nonlabeled PEO400 at room temperature in order to reduce the concentration of the spin-label to $\approx 1 \times 10^{-6}$ mol/g, using a standard solution of TEMPOL in toluene as an intensity reference. The chemical structure of SLPEO400 is shown in Chart 1.

Preparation of PEO400/Somasif Nanocomposites. PEO400/Somasif nanocomposites were prepared via the solution intercalation method.[1] Somasif was dispersed in deionized water to a concentration of 1.5 wt %. The dispersion was ultrasonicated and stirred until a homogeneous system was observed, usually for 1−3 h. SLPEO400 was dissolved in water to a concentration of 1.5 wt %, and the solution was added dropwise to the Somasif dispersion, stirred vigorously for 6 h, and followed by solvent evaporation. The sample was then dried in a vacuum oven at 333 K for 6 h. The dried sample was powdered using a mortar and pestle, dried again at 333 K for 24 h, and washed with benzene to remove the nonintercalated PEO. Our work on PEO4K/Somasif has demonstrated that only the nonintercalated PEO is removed in this procedure.[20] The nanocomposite was finally dried in a vacuum oven at 353 K for 24 h.

The amount of Somasif in the nanocomposite was determined to be 77 wt % by TGA measurement, as shown in Figure 3. The notation used for the nanocomposite is NANO(400)77. The characteristics of the samples used in this work are listed in

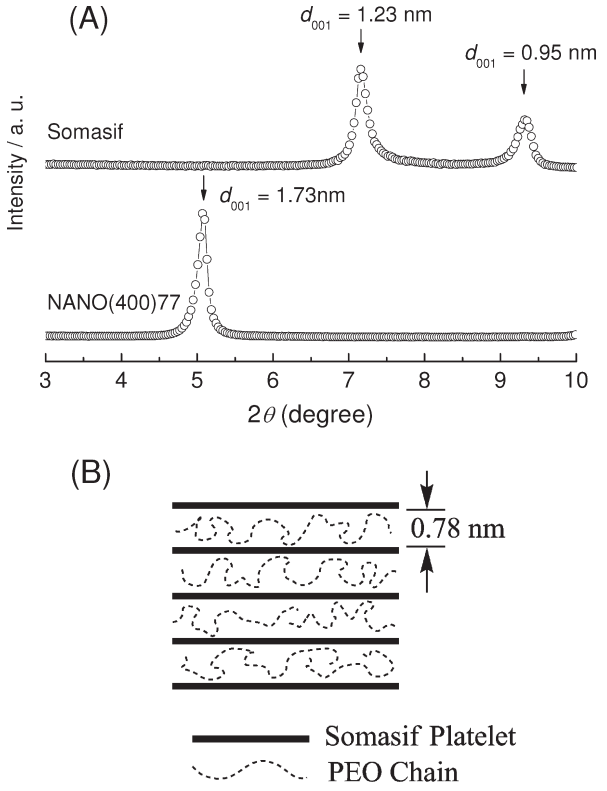

Figure 1. (A) XRD patterns of neat Somasif and NANO(400)77 in the 2θ range 3°−10°. (B) Intercalation of PEO chains in the silicate layers.

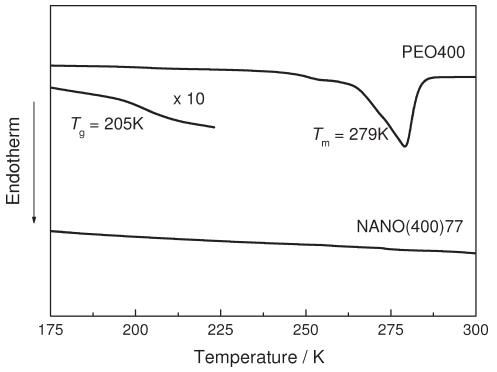

Figure 2. DSC traces for PEO400 and NANO(400)77. Note the T_g and T_m transitions for PEO400 and the absence of transitions for the nanocomposite.

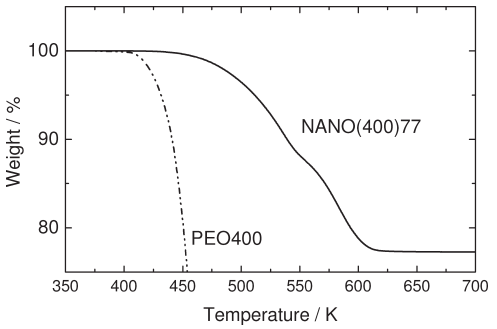

Figure 3. TGA curves of PEO400 and the nanocomposite NANO-(400)77 measured in air.

Table 1. Data for NANO82, which is an intercalated PEO4k/Somasif nanocomposite containing 82 wt % Somasif (ref 20), are also listed in Table 1.

Table 1. Characteristics of Samples Used in This Work

sample	Somasif/wt %[a]	$d_{gallery}$/nm[b]	T_g/K[c]	T_m/K[c]
PEO400			205	279
NANO(400)77	77	0.78		
NANO82[d]	82	0.83		

[a] Determined by TGA. [b] Gallery width in which PEO400 was intercalated (determined from XRD data). [c] Determined by DSC. [d] NANO82 is an intercalated PEO4k/Somasif nanocomposite referred from ref 20.

ESR Measurements. ESR samples were prepared by transferring the powders to 4 mm o.d. quartz tubes and heating under vacuum to remove the adsorbed water before sealing; SLPEO400 was heated to 333 K and NANO(400)77 to 373 K. Spectra were recorded with Bruker X-band EMX spectrometers operating at 9.7 GHz and 100 kHz magnetic field modulation and equipped with the Acquisit 32 Bit WINEPR data system version 3.01 and the ER4111 VT variable temperature unit. The microwave frequency was measured with a Hewlett-Packard 5350B microwave frequency counter. Most spectra were collected with the following parameters: sweep width 120 G, microwave power 2 mW, time constant 20.48 ms, conversion time 40.96 ms, 2−16 scans, and 2048 points. The modulation amplitude was varied in the range 0.5−2 G, depending on the line width. The temperature was controlled within ±1 K. All samples were allowed to equilibrate for at least 15 min after reaching the desired temperature.

Simulation of ESR Spectra. ESR spectra were calculated with the software based on the stochastic Liouville equation,[22] as described previously.[20] Simulated spectra were fitted to experimental spectra using a PC version of the NLSL program based on the modified Levenberg−Marquart minimization algorithm, which iterates the simulations until a minimum least-squares fit to experiment was reached.[23] The g and ^{14}N hyperfine tensors were determined by analyzing rigid-limit spectra measured at 100 K.

The model known as "microscopic order with macroscopic disorder" (MOMD) was applied for calculating the spin-label rotational diffusion.[24] The model assumes that the spin-labels undergo microscopic molecular ordering with respect to a local director; the local directors in the sample are randomly oriented in the laboratory frame. Pilar has summarized recently the successful application of the MOMD model for analyzing ESR line shapes of spin-labeled polymers.[25] The rotational diffusion of nitroxide spin-labels attached to polymer chain segments has been approximated by superposition of the isotropic rotational diffusion of the polymer chain segment with the rotational diffusion coefficient, R_S, and the internal rotation of the spin-label with the rotational diffusion coefficient, R_I.[25] When the nitroxide spin-label is attached to a polymer chain via a short tether, it is assumed that $R_{prp} = R_S$ and $R_{pll} = R_I + R_S$. Here, R_{pll} and R_{prp} are the parallel and perpendicular rotational diffusion coefficients, respectively. The use of a cylindrical symmetry for the pyrrolidine label (a five-membered ring) is justified because ESR spectra at X-band are not sensitive to fast motions such as the internal rotation of the label, which are "nearly averaged out".[24b] It appears that a rotational motional model with cylindrical symmetry is appropriate at X-band not only for a six-membered label but also for a five-membered one, as in this study. The number of parameters and the symmetry of the rotational components used in the present simulations are along the lines described in the literature for pyrrolidine spin-labels.[24b,c]

Differential Scanning Calorimetry (DSC). DSC measurements were carried out using the Q10 differential scanning calorimeter manufactured by TA Instruments, calibrated with an indium standard. Cooling was accomplished by a TA Instruments quench cooler accessory. The DSC cell was purged with dry nitrogen flowing at a rate of 50 mL/min. Measurements were carried out at a heating rate of 10 K/min.

X-ray Diffraction (XRD). Diffraction data were acquired on a Scintag X2 diffractometer using Cu Kα radiation generated at 45 kV and 40 mA and configured in a Bragg−Bretano focusing geometry. The scattering angle (2θ) was scanned at 0.03°/s in the range 3−10° using a step size of 0.03°. The Bragg equation was applied to calculate the spacing, d, of Somasif platelets.

Thermal Gravimetric Analysis (TGA). Weight loss measurements during controlled heating were carried out with TA Instruments Hi-Res TGA2950 and used to determine the amounts of residual water and polymer. Samples weighed typically ≈10 mg, and measurements were conducted during heating to 823 K at a rate of 10 K min^{-1} under flowing air.

Results

Figure 1A presents the XRD patterns for neat Somasif and NANO(400)77 measured in the 2θ range 3°−10° at ambient temperature. Somasif has two peaks, at $2\theta = 7.2°$ ($d_{001} = 1.23$ nm) and 9.3° (0.95 nm), indicating hydrated and dehydrated phases, respectively.[26] NANO(400)77 shows a peak at $2\theta = 5.1°$ ($d = 1.73$ nm). The increase of d is attributed to the intercalation of PEO400 into clay galleries: The gallery in which PEO400 is intercalated is 0.78 nm in the NANO(400)77 (1.73−0.95 nm), as shown in Figure 1B. DSC traces of PEO400 and NANO(400)77 are shown in Figure 2, where melting and glass transitions for PEO400 appear at 279 and 205 K, respectively. The degree of crystallinity of PEO400 is estimated to be ≈52% using 222.2 J/gas as the fusion enthalpy of PEO crystallites[27] while the crystallinity of PEO4k is 91%, most likely because of the high concentration of chain ends. No transitions were detected for NANO(400)77. The weight loss (TGA) data for PEO400 and NANO(400)77 shown in Figure 3 clearly show that NANO(400)77 has a decomposition temperature ≈100 K higher than PEO400.

Selected experimental and simulated ESR spectra of SLPEO400 and NANO(400)77 in the range 100−410 K are shown in Figure 4. The temperature dependence of the ESR line shapes is due to changes in the rotational rate of the nitroxide radical with correlation time, τ_c, defined as $1/(6(R_{prp}{}^2 R_{pll})^{1/3})$. The rigid-limit spectra observed at 100 K were successfully fitted using the NLSL program with very slow isotropic Brownian rotational diffusion of the spin-label ($R_{pll} = R_{prp} = 1 \times 10^3$ s^{-1}). Best fits required a superposition of Lorentzian line shape with Gaussian inhomogeneous broadening. The Gaussian line width is considered to reflect local interactions sensed by the nitroxide labels. The Gaussian and Lorentzian line widths (ΔH_G and ΔH_L) and the A and g tensors used for the best fits are listed in Table 2. The A_{zz} values were determined from experimental spectra within ±0.1 G. The A and g tensors were fixed for the simulations at the higher temperatures.

R_S, R_I, and the other parameters describing the local dynamics in the PEO chains were determined by fitting experimental spectra, and the results are shown in Figure 5. ESR spectra of SLPEO400 were simulated with a single spectral component, but two different spectral components, fast and slow, were necessary to fit the spectra for NANO(400)77. Arrhenius plots of R_S and R_I are shown in parts A and B of Figure 5, and the corresponding activation energies E_S and E_I are listed in Table 3. The R_S values for SLPEO4K and for NANO82 (from ref 20) are also plotted in Figure 5A; NANO82 is an intercalated PEO4K/Somasif nanocomposite containing 82 wt % Somasif. The percentages of the fast component in NANO(400)77 and NANO82 are compared in Figure 6.

The effect of the dynamic parameters on the simulated line shapes was investigated in detail. The variation of the parameters R_{prp}, R_{pll}, β_D, c_{20}, and c_{22} is shown in the Supporting Information and compared to the best-fitting simulated spectrum. The line shapes are very sensitive to the dynamic parameters, indicating the narrow range of the parameters that can be deduced and that characterize the dynamics in these systems.

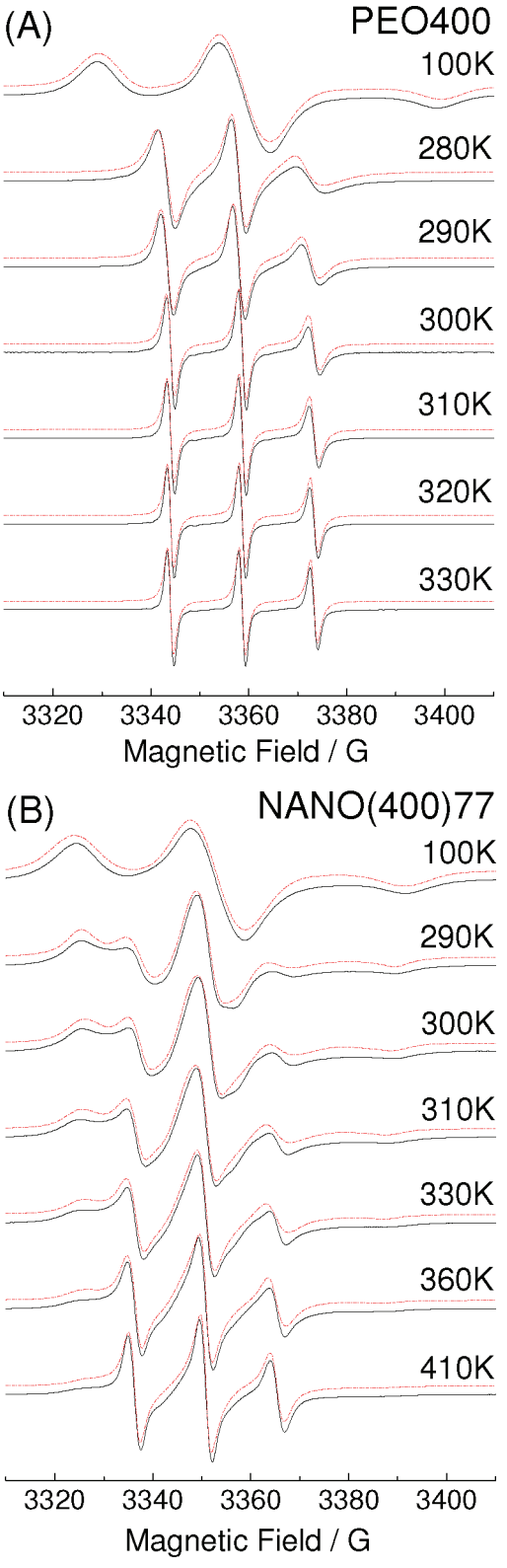

Figure 4. Temperature variation of experimental (—) and simulated (---) ESR spectra for (A) SLPEO400 and (B) NANO(400)77.

Discussion

Structure of NANO(400)77. The XRD data shown in Figure 1 indicate that the polymer is intercalated in clay galleries of width 0.78 nm (1.73−0.95 nm) in NANO(400)77,

Table 2. Parameters Used for the Simulation of ESR Spectra

sample	g_{xx}	g_{yy}	g_{zz}	A_{xx}/ G	A_{yy}/ G	A_{zz}/ G	ΔH_G/ G	ΔH_L/ G
PEO400	2.0087	2.0067	2.0020	5.5	3.7	34.8	7.0	1.5
NANO(400)77	2.0088	2.0067	2.0025	5.9	4.2	33.6	8.6	1.4

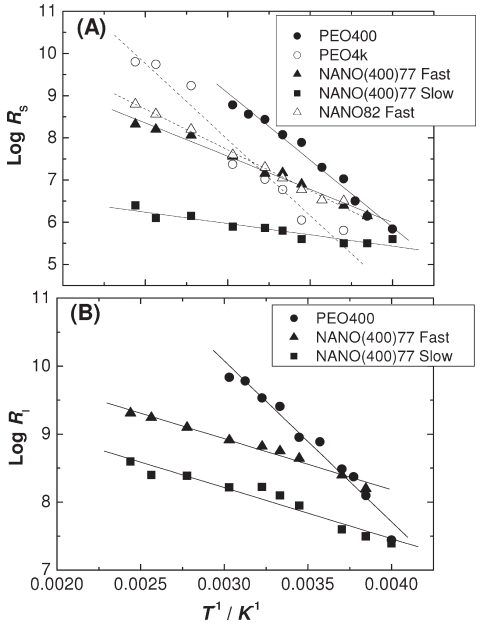

Figure 5. Arrhenius plots of the rotational diffusion coefficients R_S in (A) and R_I in (B). Data for PEO4K and NANO82 are from ref 20.

Table 3. Activation Energies

sample	E_S/kJ mol^{-1}	E_I/kJ mol^{-1}
PEO400	61	45
NANO(400)77 (slow component)	10	14
NANO(400)77 (fast component)	30	14

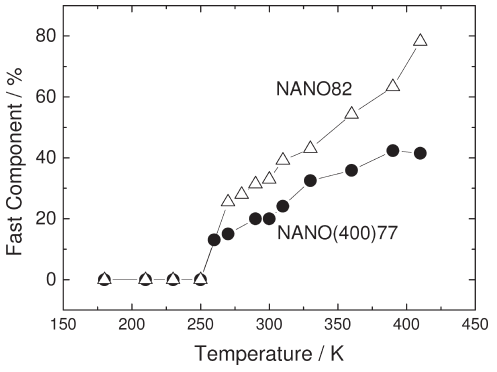

Figure 6. Temperature variation of the relative intensity (%) of the fast spectral component in NANO(400)77. Data for NANO82 are from ref 20.

as illustrated in Figure 1B. The thickness of a PEO chain containing only trans bonds was reported to be about 0.37 nm.[8] The aggregation of PEO chains is disturbed in the gallery because of limited space. As reported in our previous paper, the gallery width in NANO82 is 0.83 nm.[20] Therefore, PEO400 is confined in slightly narrower galleries compared to PEO4K.

NANO(400)77 did not show any transitions in the DSC trace in contrast to that the PEO400 showed melting and glass transitions at 279 and 205 K, respectively (Figure 2). The absence of the melting transition indicates that the crystallization of PEO400 is inhibited in the galleries. Moreover, it also indicates that segmental cooperative motions of intercalated PEO400 are hindered because a glass transition is a relaxation mode based on segmental cooperative motions.[16] In the bulk state, the length scale of the cooperativities near the glass transition was determined to be a few nanometers.[28] These results are in good agreement with the previously reported DSC results for the PEO/clay nanocomposites.[6,20]

NANO(400)77 showed significantly higher decomposition temperature than bulk PEO400 (Figure 3). Polymer/clay nanocomposites usually show higher degradation temperature compared to bulk polymers because the diffusion of oxygen molecules is disturbed by the clay platelets.[29] Results in Figure 3 provide additional evidence for the intercalation of PEO chains in the galleries.

Hindered Hydrogen Bonding in the Galleries. ESR spectra at 100 K reflect the local environment around the labeled chains because their motion is frozen. It is well-known that the A_{zz} value is sensitive to, and increases with, the local polarity.[30,31] For SLPEO400 A_{zz} = 34.8 G, remarkably larger than that of the SLPEO4K, 33.6 G,[20] due to the high concentration of hydroxyl groups at the chain ends in PEO400. The increase in the hydroxyl group concentration increases the polarity of PEO; a hydroxyl group forms a hydrogen bond with a nitroxide, and the result is a significant A_{zz} increase.[32] In other words, the nitroxide labels are good indicators for local polarity and hydrogen bonding.

For NANO(400)77 A_{zz} = 33.6 G, significantly smaller than that of bulk SLPEO400 (34.8 G), suggesting a decrease in the hydroxyl group concentration around the nitroxide labels. Therefore, the hindered hydrogen bonding between the hydroxyl groups and the nitroxide labels in the galleries is considered to be the main factor of the small A_{zz} value for NANO(400)77. Moreover, the A_{zz} value of NANO(400)77, 33.6 G, is almost the same as that of NANO82, 33.4 G.[20] Namely, the hydroxyl group concentration around the nitroxide labels did not increase even though the number of hydroxyl groups increased in the galleries. This result indicates that the PEO segments in the galleries are isolated, and the interactions between PEO segments are negligible.

Segmental Mobility of PEO in Clay Galleries. NANO(400)77 showed two motional components, fast and slow, in contrast to the single motional component in SLPEO400. As discussed in our previous work, the fast and slow motional components can be attributed to PEO segments weakly and strongly interacting with the solid surface.[20] This conclusion is in accord with computer simulations, which showed the coexistence of fast and slow segmental relaxations and determined a higher segmental density with a slower segmental relaxation near the platelet surface.[9,12,15] Moreover, as shown in Figure 6, our experimental results also showed an increase in the intensity of the fast motional component with an increase in temperature, in accord with the prediction of the computer simulations. NANO(400)77 showed a lower percentage of the fast motional component than NANO(4k)82 (Figure 6), indicating that more PEO segments are strongly interacting with the platelet surface in NANO(400)77 compared to NANO82. As described above, the gallery in the NANO(400)77 (0.78 nm) is narrower than in NANO(4k)82 (0.83 nm). It is expected that PEO segments interact more strongly with the platelet surface in narrower galleries. In fact, when PEO4K was intercalated in 0.33 nm galleries, no fast motional component was observed.[20] These results indicate that the mobility of confined PEO chains increases with an increase in the gallery width because more PEO segments are released from the attractive interactions between PEO segments and the

platelet surface. We can therefore expect that the hydroxyl terminals form hydrogen bonding with the silicate surface; therefore, the mobility in NANO(400)77 is lower than in NANO82 because the chain ends act as immobilized anchoring points. However, FT-IR spectra measured at ambient temperature showed that the O−H stretching vibration at 3333 cm^{-1} in PEO400 is shifted to higher frequency in NANO(400)77 (Figure S-4). This surprising result indicates that the interactions with the hydroxyl groups are weakened in the galleries; therefore, the chain ends are not acting as immobilized chain ends.

The log R_S value of the fast motional component in NANO(400)77 is lower than that of SLPEO400, as shown in Figure 5A. For example, log R_S for NANO(400)77 and for SLPEO400 at 330 K are 7.6 and 8.8, respectively. This result indicates that the motional rate of the PEO segments is slower in the galleries because of the attractive interactions between PEO segments and the platelet surface. This logic can also rationalize the recent reduced segmental mobility of PEO chains confined in nanometer thick laponite galleries, as reported recently by Lorthioir et al. in their ^{13}C and ^{1}H solid-state NMR study.[11]

On the other hand, the E_S value of the fast motional component in NANO(400)77 (30 kJ/mol) is lower than that of bulk PEO400 (61 kJ/mol) (Table 3). In the bulk, polymer segments move cooperatively with neighboring segments.[16] It is expected that the activation energy of the segmental motion increase with increases in the size and strength of the cooperativity. However, segmental cooperative motions of SLPEO400 are hindered in the galleries, as suggested by the absence of the glass transition in NANO(400)77 by DSC. Therefore, we suggest that the lower value of E_S for the fast motional component in NANO(400)77 is due to the hindered segmental cooperative motion in the galleries. A lower activation energy for the intercalated PEO was also detected by TSC[6] and dielectric relaxation[13,14] measurements.

Effect of the Molecular Weight on PEO Dynamics in Clay Galleries. The glass transition temperature of a polymer generally decreases with an increase in the concentration of chain ends in chains with lower molecular weights.[33] Because the spin-labeled sites move cooperatively with neighboring segments in the bulk, the mobility of the spin-labeled sites increases with an increase in the chain end concentration even when the chain ends are spin-labeled.[34,35] In contrast, if the cooperative motion with neighboring segments is hindered, the mobility of the spin-labeled sites is *not* enhanced with a decrease in the molecular weight.

PEO400 has a higher mobility than PEO4K (Figure 5A) because of the higher chain end concentration. This result indicates that the molecular mobility of the spin-labeled sites was enhanced by the chain ends through the cooperative motions. On the other hand, NANO(400)77 showed somewhat lower mobility than NANO(4k)82: For example, the log R_S values of the fast motional component in the NANO(400)77 and NANO82 at 410 K were 8.3 and 8.8, respectively (Figure 5A). Taking into account the narrower galleries in the NANO(400)77, stronger attractive interactions between the PEO segments and the platelet surface are expected for the NANO(400)77; this is considered as the cause of the lower mobility in NANO(400)77. Furthermore, this result indicates that the mobility of the spin-labeled sites of the intercalated PEO was *not* enhanced by the increased chain ends. This is new evidence for the idea that the cooperative segmental motion of PEO is reduced in the galleries.

Ordering Potentials. Best fits of ESR spectra were achieved with ordering potential parameters c_{20} and c_{22}, which describe the shape of the ordering potential at a given temperature.[24d] The combination of positive c_{20} and c_{22} values results in a maximum in the director orientation distribution in the $\mathbf{x}_R-\mathbf{z}_R$ plane.[24d] For PEO400, c_{22} is sensitive to the temperature and much larger than c_{20} (Figure S-1); above ca. 280 K, both c_{20} and c_{22} values become close to zero, indicating a random rotational diffusion of the labels. In this temperature regime the label motion is activated by the segmental motion of PEO.[20] We note that in this study the chain end of the PEO was labeled. The motion of the chain end is expected to be more isotropic than the inner segments. Therefore, the motional ordering of the labels becomes almost isotropic as the label motion is activated by the segmental motion of the PEO main chain. The ordering potential parameters for the NANO(400)77 show a similar tendency with that of the PEO400: the behavior of the local motion around the label for the fast motional components in NANO(400)77 is similar to that in bulk PEO.

Conclusions

The effect of chain ends on the dynamics of PEO intercalated in Somasif galleries was investigated by comparing PEO400 and PEO4K. For the bulk polymers, PEO400 showed much higher mobility than PEO4K because of the higher chain end concentration. The molecular mobility of the spin-labeled sites is enhanced by mobile chain ends through the cooperative motion with neighboring segments. On the other hand, the mobility of the spin-labeled sites of the intercalated PEO was not enhanced by the increased number of chain ends. This result indicates that the cooperative segmental motions are reduced in the galleries. Moreover, the lower A_{zz} value of the NANO(400)77 compared to that of PEO400 indicates hindered hydrogen bonding between hydroxyl groups at the chain ends and nitroxide labels in the galleries. From these results, we conclude that interactions between PEO segments are negligible.

Acknowledgment. This study was supported by the Polymers Program of the National Science Foundation. The authors thank CO-OP Chemical, Japan, for the gift of the Somasif ME-100 and are grateful to Professor D. E. Budil for his kind guidance on MOMD simulations. The careful reading of the manuscript and the constructive criticism of the two reviewers is greatly appreciated.

Supporting Information Available: Temperature dependence of c_{20} and c_{22} for PEO400 and NANO(400)77 (Figure S-1); effects of parameter variation on the simulated spectra of PEO400 and NANO(400)77 (Figures S-2 and S-3, respectively); FT-IR spectra of PEO400 and NANO(400)77 (Figure S-4). This material is available free of charge via the Internet at http://pubs.acs.org.

References and Notes

(1) Aranda, P.; Ruiz-Hitzky, E. *Chem. Mater.* **1992**, *4*, 1395–1403.
(2) Wu, J.; Lerner, M. M. *Chem. Mater.* **1993**, *5*, 835–838.
(3) Wong, S.; Vasudevan, S.; Vaia, R. A.; Giannelis, E. P.; Zax, D. B. *J. Am. Chem. Soc.* **1995**, *117*, 7568–7569.
(4) Wong, S.; Vaia, R. A.; Giannelis, E. P.; Zax, D. B. *Solid State Ionics* **1996**, *86−88*, 547–557.
(5) Krishnamoorti, R.; Vaia, R. A.; Giannelis, E. P. *Chem. Mater.* **1996**, *8*, 1728–1734.
(6) Vaia, R. A.; Sauer, B. B.; Tsu, O. K.; Giannelis, E. P. *J. Polym. Sci., Part B: Polym. Phys.* **1997**, *35*, 59–67.
(7) Harris, D. J.; Bonagamba, T. J.; Schmit-Rohr, K. *Macromolecules* **1999**, *32*, 6718–6724.
(8) Bujdák, J.; Hackett, E.; Giannelis, E. P. *Chem. Mater.* **2000**, *12*, 2168–2174.
(9) Hackett, E.; Manias, E.; Giannelis, E. P. *Chem. Mater.* **2000**, *12*, 2161–2167.

(10) Chen, B.; Evans, J. R. G. *J. Phys. Chem. B* **2004**, *108*, 14986–14990.
(11) Lorthioir, C.; Lauprêtre, F.; Soulestin, J.; Lefebvre, J.-M. *Macromolecules* **2009**, *42*, 218–230.
(12) Kuppa, V.; Menakanit, S.; Krishnamoorti, R.; Manias, E. *J. Polym. Sci., Part B: Polym. Phys.* **2003**, *41*, 3285–3298.
(13) Elmahdy, M. M.; Chrissopoulou, K.; Afratis, A.; Floudas, G.; Anastasiadis, S. H. *Macromolecules* **2006**, *39*, 5170–5173.
(14) Chrissopoulou, K.; Afratis, A.; Anastasiadis, S. H.; Elmahdy, M. M.; Floudas, G.; Frick, B. *Eur. Phys. J. Spec. Top.* **2007**, *141*, 267–271.
(15) Kuppa, V.; Manias, E. *J. Chem. Phys.* **2003**, *18*, 3421–3429.
(16) Adam, G.; Gibbs, J. H. *J. Chem. Phys.* **1965**, *43*, 139–146.
(17) Brik, M. E.; Titman, J. J.; Bayle, J. P.; Judeinstein, P. *J. Polym. Sci., Part B: Polym. Phys.* **1996**, *34*, 2533–2542.
(18) Panek, G.; Schleidt, S.; Mao, Q.; Wolkenhauer, M.; Spiess, H. W.; Jeschke, G. *Macromolecules* **2006**, *39*, 2191–2200.
(19) Miwa, Y.; Drews, A. R.; Schlick, S. *Macromolecules* **2006**, *39*, 3304–3311.
(20) Miwa, Y.; Drews, A. R.; Schlick, S. *Macromolecules* **2008**, *41*, 4701–4708.
(21) Finnigan, B.; Jack, K.; Campbell, K.; Halley, P.; Truss, R.; Casey, P.; Cookson, D.; King, S.; Martin, D. *Macromolecules* **2005**, *38*, 7386–7396.
(22) Schneider, D. J.; Freed, J. H. In *Biological Magnetic Resonance*; Berliner, L. J., Reuben, J., Eds.; Plenum: New York, 1989; Vol. *8*, Chapter 1, pp 1−76.
(23) Budil, D. E.; Lee, S.; Saxena, S.; Freed, J. H. *J. Magn. Reson. A* **1996**, *120*, 155–189.
(24) (a) Meirovitch, E.; Nayeem, A.; Freed, J. H. *J. Phys. Chem.* **1984**, *88*, 3454–3465. (b) Xu, D.; Budil, D. E.; Ober, C. K.; Freed, J. H. *J. Phys. Chem.* **1996**, *100*, 15867–15872. (c) Liang, Z.; Freed, J. H. *J. Phys. Chem. B* **1999**, *103*, 6384–6396. (d) Earle, K. A.; Budil, D. E. In *Advanced ESR Methods in Polymer Research*; Schlick, S., Ed.; Wiley: Hoboken, NJ, 2006; Chapter 3, pp 53−83.
(25) Pilar, J. In *Advanced ESR Methods in Polymer Research*; Schlick, S., Ed.; Wiley: Hoboken, NJ, 2006; Chapter 6, pp 133−163 and references therein.
(26) Maiti, P. *Langmuir* **2003**, *19*, 5502–5510.
(27) Braun, W.; Hellwege, K.-H.; Knappe, W. *Kolloid Z. Z. Polym.* **1967**, *215*, 10–15.
(28) Rizos, A. K.; Ngai, K. L. *Phys. Rev. E* **1999**, *59*, 612–617.
(29) Ajayan, P. M.; Schadler, L. S.; Braun, P. V. *Nanocomposite Science and Technology*; Wiley-VCH: Germany, 2004.
(30) Griffith, O. H.; Jost, P. C. In *Spin Labeling Theory and Applications*; Berliner, L. J., Ed.; Academic Press:New York, 1976; p 453.
(31) Griffith, O. H.; Dehlinger, P. J.; Van, S. P. *J. Membr. Biol.* **1974**, *15*, 159–192.
(32) Jeschke, G. In *Advanced ESR Methods in Polymer Research*; Schlick, S., Ed.; Wiley: Hoboken, NJ, 2006; Chapter 7, pp 165−195.
(33) Fox, T. G.; Flory, P. J. *J. Appl. Phys.* **1950**, *21*, 581–591.
(34) Miwa, Y.; Tanase, T.; Yamamoto, K.; Sakaguchi, M.; Sakai, M.; Shimada, S. *Macromolecules* **2003**, *36*, 3235–3239.
(35) Miwa, Y.; Yamamoto, K.; Sakaguchi, M.; Sakai, M.; Makita, S.; Shimada, S. *Macromolecules* **2005**, *38*, 832–838.